Simulation of neural population dynamics with a refractory density approach and a conductance-based threshold neuron model

Anton V. Chizhov[a,*,1], Lyle J. Graham[a], Andrey A. Turbin[b]

[a]*Laboratory of Neurophysics and Physiology, UMR 8119 CNRS, University Paris-5, 45 rue des Saint-Peres, 75006 Paris, France*
[b]*Radio-Physics Department, St. Petersburg State Polytechnic University, Polytekhnicheskaya 29, 195251 St.-Petersburg, Russia*

Abstract

We propose a macroscopic approach towards realistic simulations of population activity of cortical neurons, based on the known refractory density equation and a new threshold model of neuronal firing. The threshold model is a Hodgkin–Huxley model that is reduced by omitting the fast sodium current and instead using an explicit threshold criterion for action potential events based on the derivative of the membrane potential. The membrane potential of the model realistically describes postspike refractory states and postsynaptic current integration. The dynamics of a neural continuum are thus described by a partial differential equation in terms of the distributions of the refractory density, where the refractory state is defined by the time elapsed since the last action potential, the membrane potential and the potassium conductance, across the entire population. As a source term in the density equation, a probability density of firing, or a hazard function, is derived from the equation assuming a Gaussian distribution of spike thresholds over the population. Responses of an ensemble of unconnected neurons to stimulation by current step and sinusoidal inputs are simulated and compared with simulations of discrete individual neurons. A synaptically connected population model is also evaluated and compared with a model network of discrete neurons.
© 2006 Elsevier B.V. All rights reserved.

Keywords: Neuron ensemble; Population model; Refractory density equation; Hodgkin–Huxley model; Threshold model

1. Introduction

Individual cortical neurons operate within the background activity of neuron populations occupying large areas of the cortex. Relative to the single-cell activity this background activity is macroscopic, and therefore calls for independent approaches for its mathematical description. Whereas detailed single-neuron models are well developed, there is no generally accepted biophysically meaningful macroscopic model of neuronal ensemble activity. Our approach considering a neural ensemble as a continuum in a state parameter space is based on the ideas and methods introduced in [9,18,23]. Similar approaches have been described in [11], where a review of the theories based on the notion of a probability density function can be found. However, the implementation of this theory proposed here, based on a reduced and experimentally constrained single-neuron conductance-based model, appears to be novel.

We apply the probability density approach (PDA) to describe an infinite number of similar neurons as a continuum. In contrast to population models of the firing rate type [5,8,20,21,26], which are valid only for quasi-stationary states of ensemble activity, a PDA can take into account the relaxation properties of neurons and thereby correctly calculate the firing rate in non-stationary dynamical regimes [9]. In particular, the PDA presented here describes the evolution of a neuronal continuum in the phase space (PS) of a specific choice of neuronal state variables. In general, if we consider the Hodgkin–Huxley type conductance-based model of a single neuron, the state variables include the membrane potential and those

*Corresponding author. Tel.: +33 1 42862087.

E-mail address: Anton.Chizhov@mail.ioffe.ru (A.V. Chizhov).

[1]Permanent position: A.F. Ioffe Physico-Technical Institute of RAS, 26 Politekhnicheskaya str., 194021 St.-Petersburg, Russia.

describing the ionic current conductances. To simulate macroscopic processes in cortical tissue, such as extra-cellularly evoked excitation of large populations of cortical neurons, synchronized oscillations or traveling waves, a model must reproduce stationary and non-stationary modes of neuronal firing, as well as the effects of refractoriness and, when present, the effects of slow ionic currents. These considerations are possible in the frame of a single-neuron model of the Hodgkin–Huxley type.

However, the large number of associated parameters for the Hodgkin–Huxley model necessarily complicates the equations for the ensemble dynamics. This is a major reason that many approaches consider only one state variable, the membrane potential, governed by the integrate-and-fire or by the spike response model (SRM) (e.g. [17]). Nevertheless, the membrane potential is only a weak predictor of the neuron's complete state, primarily because neurons with different refractory states can have the same potential. On the other hand, the time elapsed since the last action potential approximates the refractory state quite well. This relationship motivates a refractory density approach [9,11], which considers the evolution of a neuronal density distribution in the space of single parameter, the time elapsed since the last spike, as a particular case of the PDA.

The key element of the present work is that of implanting a conductance-based neuron model into the PDA. To this end, we first develop a threshold version of the experimentally constrained Hodgkin–Huxley-like model, and we then derive the appropriate refractory density equation (RDE) for this model.

The value of the threshold potential in a biological neuron is a dynamic variable that depends on the current state of cell. The threshold model is obtained in Section 2.1 by omitting the fast sodium current from the Hodgkin–Huxley equations, and in its place introducing a threshold criterion that depends on the derivative of the membrane potential. The corresponding membrane potential is referred as the averaged sub-threshold potential over the neurons of a given population, under the assumption that the input current is equal for all neurons. Advantages of the model in comparison with the integrate-and-fire and SRM are outlined in this section and in the Discussion.

The approximation of the threshold as a function of the potential slope in the present model is obtained by comparing the solutions by the both biophysically detailed and reduced single-neuron models in Section 2.2.

In Section 2.3 we write the equations of the refractory density approach, or RDE. We have chosen the RDE as a simple and precise PDA which distinguishes different neurons in an ensemble by the time interval since their last spike. The probability density in the space of this interval is referred to as a refractory density [11]. In the PDA neurons are grouped into large populations of similar neurons. For each population, we form a probability density that represents the distribution of neurons across all possible states. The most complete version of this model describes the state of a neuron with as many state variables as the corresponding single-neuron model. In the simple version of this model that is presented here, the state variables of a neuron are assumed to be dependent on only one parameter, that is the time elapsed since the last spike. This parametrization reduces the dimension of the PS of states of the classical Hodgkin–Huxley neuron from four to one, yielding a set of one-dimensional partial differential equations. We calculate the membrane potential and potassium conductance, along with the refractory density, by means of the threshold-Hodgkin–Huxley-based model mentioned above, which serve to define the term governing neural excitation in the RDE, referred to in [11] as the hazard function.

The differences in intrinsic properties between neurons within the given population, as well as fluctuations of any stochastic currents affecting the neurons, are taken into account by a distribution of threshold potentials. In Section 2.4 we assume this distribution to be Gaussian (though the derivations can be carried out for more general distributions). With this distribution of the threshold potentials, the firing probability density or the hazard function as the source term in the RDE is derived.

In Section 3 we present the results of single population simulations and comparison with simulations of an ensemble of non-interacting neurons. We discuss the results in Section 4.

2. Governing equations

Our implementation of the population density approach is based on a threshold model constructed from the conductance-based single-neuron model. Although the approach could be generalized or reduced to other simplified-neuron models, (see [18,17,11]), the population model based on the proposed threshold neuron model is low-dimensional, computationally efficient, biophysically meaningful and matched to experiments. Based on the threshold neuron, we then make a main assumption that the state variables of the neuron are parameterized by a single parameter, the time elapsed since the last spike, which in turns allows the one-dimensional population density description.

2.1. Single-neuron model

We now consider a single-compartment conductance-based neuron model with Hodgkin–Huxley-like approximations of the individual voltage-dependent currents. The membrane potential $V(t)$ is governed by the equation

$$C\,\mathrm{d}V/\mathrm{d}t = -I_{\mathrm{Na}} - I_{\mathrm{K}} - I_{\mathrm{L}} - I_{\mathrm{i}}, \tag{1}$$

where the transmembrane current is, for simplicity, assumed to be a sum of only sodium and potassium voltage-dependent currents, I_{Na} and I_{K}, the leak current I_{L} and a synaptic or injected intracellular current I_{i}. We approximate the voltage-dependent currents according to

[24]. According to this approximation, the sodium current activation is instantaneous ($m(V) = m_\infty(V)$), which allows associating the threshold potential with the sodium current activation potential, and helps to compare models in Section 3. In comparison to the parameters used in [24], we set the maximum potassium conductance $\overline{g}_K = 40\,\mathrm{ms/cm^2}$, and we assume the membrane area is equal to $0.01\,\mathrm{mm^2}$.

To obtain the threshold neuron model we note that the primary role for the sodium current is for pulse generation, and assume that it has only a weak influence on the membrane current between spikes (Fig. 1). Accordingly, we define a subthreshold potential $U(t)$ as the membrane potential of the neuron with the sodium current eliminated, i.e. according to the equation

$$C\,\mathrm{d}U/\mathrm{d}t = -I_K - I_L - I_i. \tag{2}$$

Below, in Section 2.2, we find the threshold value $\overline{V^T}$ for U. When the potential U reaches the threshold $\overline{V^T}$, it is reset to the value U^{reset} chosen to be equal to $-40\,\mathrm{mV}$. The gating variable for the potassium current, $n_K^{reset} = 0.45$, was
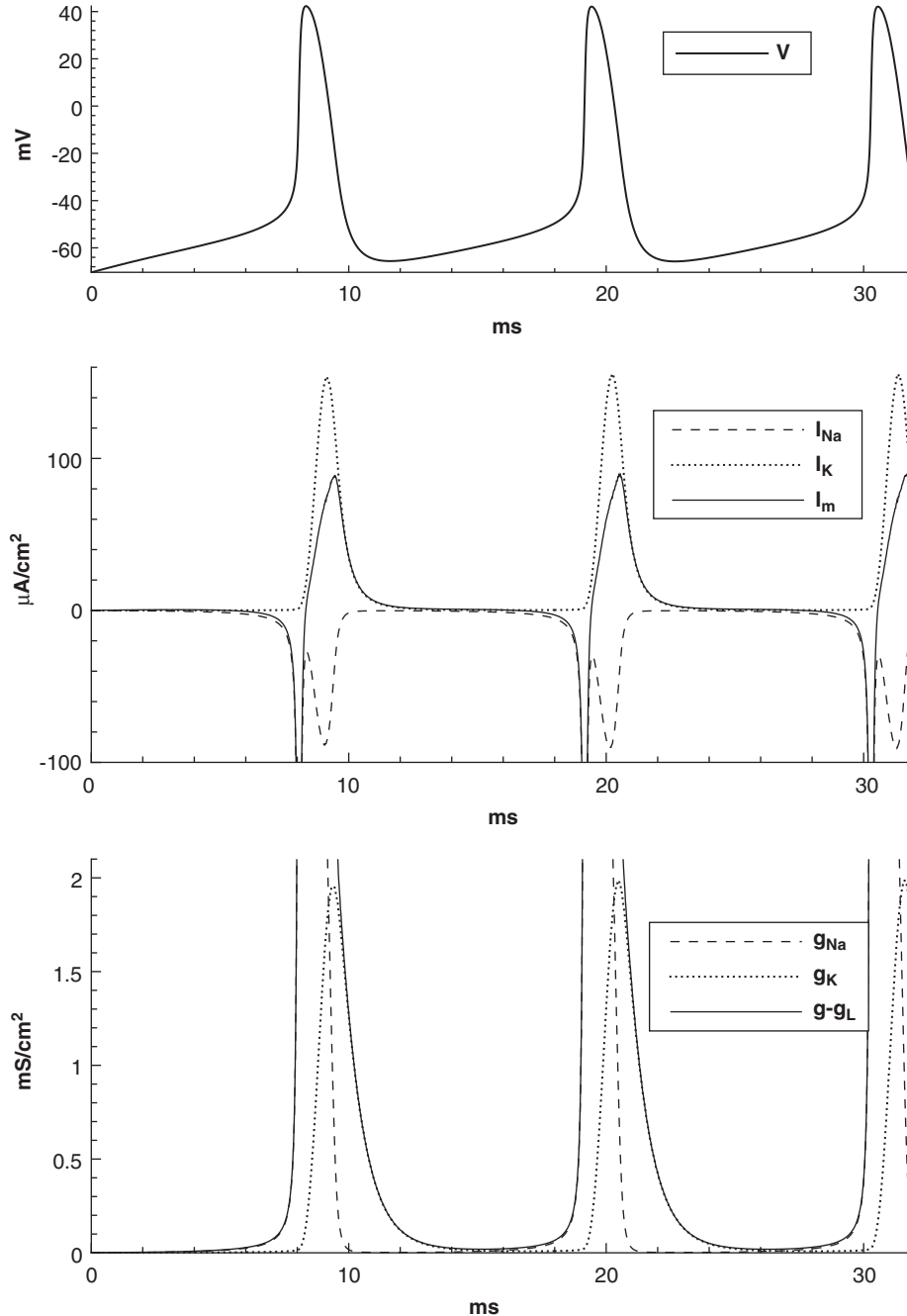

Fig. 1. The membrane potential, ionic currents and ionic conductances in the Hodgkin–Huxley-like model [24] with $I_i = 300\,\mathrm{pA}$; I_m is the total membrane current except I_i, i.e. $I_m = I_{Na} + I_K + I_L$. Note that the significant role for the sodium current is for pulse generation, and it does not have a strong influence on the potential between spikes.

measured at the descending phase of a spike, when $U = U^{\text{reset}}$ in the full model based on (1). The membrane potential and the gating variable n_K are kept constant following the threshold crossing for a duration $\Delta t_{\text{AP}} = 1.4$ ms, corresponding to the duration of the action potential. After this delay, the sub-threshold potential U accounts for the postspike refractory period due to the potassium current, according to the assumption that any contribution to the membrane potential during the refractory period from the sodium current is negligible. Since the potential U satisfactorily approximates the potential V on the interspike intervals, with properly derived threshold criteria we can accurately calculate the spike times.

In contrast to an integrate-and-fire neuron, the proposed model automatically gives the refractory period and its dependence on the strength of stimulating current. An essential aspect of this model for the population density approach is that given a subset of neurons with the same input current and time since last spike, until a subsequent spike the potential U of all the neurons in the subset is uniquely defined and identical. Thus, the potential U can be parameterized by the time passed since the last spike.

Note that this method can readily take into account other ionic currents, for example a slow after-hyperpolarization (AHP) current governed by the firing rate of a neuron [6].

We now define the firing threshold for the potential U.

2.2. Average threshold $\overline{V^{\text{T}}}$

The kinetics of the sodium channel depends on both the instantaneous value of the potential and its history. Here we rely on the simplest description of this dependence in terms of the functional expression of the sodium current, the action potential, by characterizing the average threshold $\overline{V^{\text{T}}}$ as a function of the dU/dt. To calculate this dependence we use both the Hodgkin–Huxley model (1) and its reduction (2). The dependence is obtained by applying different current steps I_i and solving Eqs. (1) and (2) for the exact, $V(t)$, and subthreshold, $U(t)$, potentials, respectively (Fig. 2A). We then define the threshold as the value of the potential U at the spike maximum for the potential V, i.e. at $t = t_{\text{AP}}$; this value $\overline{V^{\text{T}}} = U|_{t=t_{\text{AP}}}$, and the corresponding $dU/dt|_{t=t_{\text{AP}}}$, gives one point of the desired threshold function

$$\overline{V^{\text{T}}} = \overline{V^{\text{T}}}(dU/dt) \tag{3}$$

shown in Fig. 2B. This dependence satisfactorily approximates the threshold in the case of arbitrary stimulation. For example, for an input current oscillating at 10 Hz the maximum error of the predicted threshold was found to be approximately 1.5 mV.

Using the estimated dependence of spike threshold on the voltage derivative the threshold model based on Eq. (2) is completed. This model gives correct spike times for both
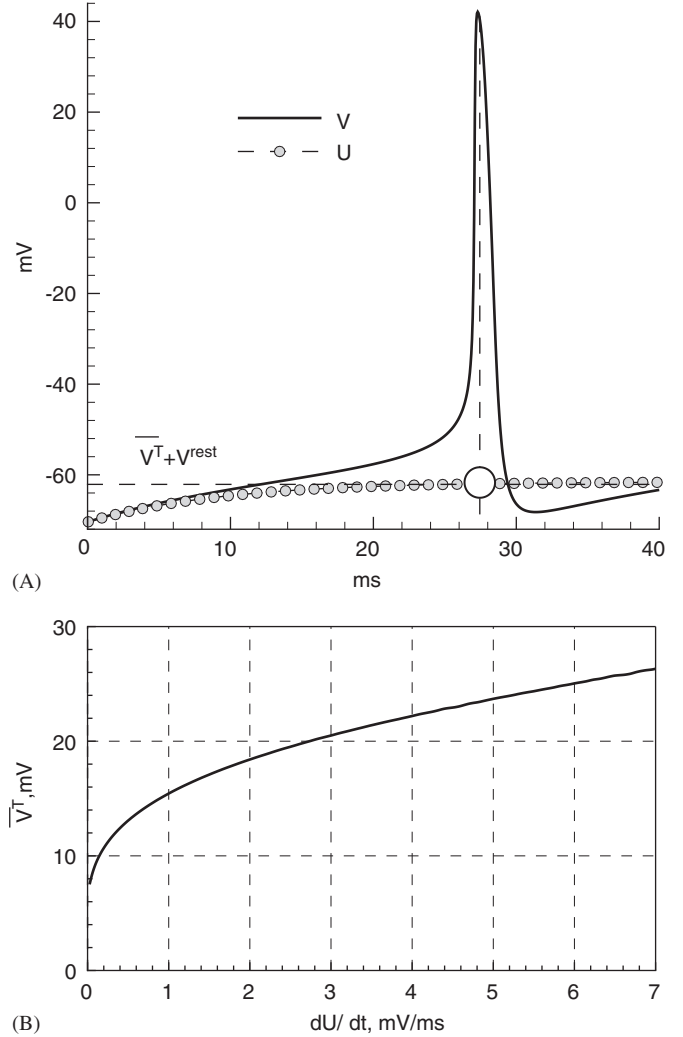

Fig. 2. The threshold potential $\overline{V^{\text{T}}}$ as a function of the potential slope dU/dt is calculated, comparing the solutions of Eqs. (1) and (2). (A) The solutions obtained by the complete Hodgkin–Huxley model and the threshold model for $V(t)$ and $U(t)$, correspondingly, given the injected current $I_i = 100$ pA. The value of U at the instant of the spike peak gives the threshold potential $\overline{V^{\text{T}}}$. (B) The calculated dependence of the threshold potential on the sub-threshold potential slope $\overline{V^{\text{T}}} = \overline{V^{\text{T}}}(dU/dt)$.

the first and subsequent spikes in a spike train in response to a constant current step, when compared to the full Hodgkin–Huxley model. The spike time precision for arbitrary stimuli is better than that of an integrate-and-fire model with fixed artificial refractory period, threshold and reset potential (Fig. 3) and maintains this precision for different stimulation amplitudes.

In comparison to the threshold dependence on the voltage rate presented here, it has been proposed (e.g. [13,15]) that a dynamic threshold relaxes after the spike from a reset value to its steady-state level, according to a first order differential equation. In terms of the time elapsed since the last spike, t^*, this rule may be expressed as a function $\overline{V^{\text{T}}} = f(t^*)$, where f is an exponentially decreasing function. Thus, although this approach
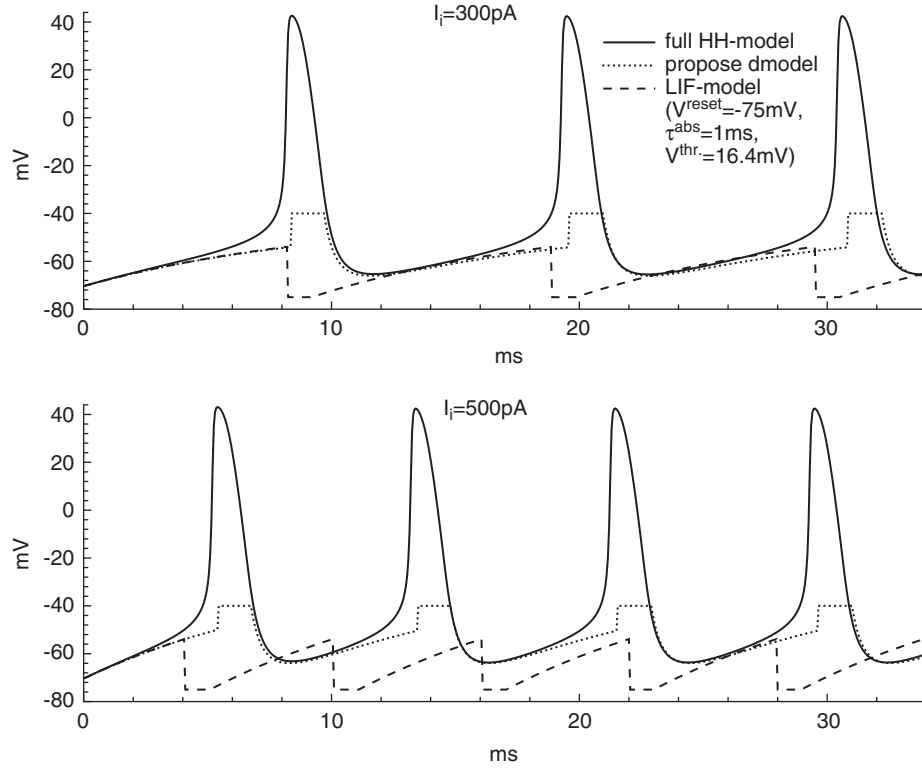
Fig. 3. Comparison of spike times predicted by the proposed threshold model and linear integrate-and-fire model with the full Hodgkin–Huxley model in the cases of $I_i = 300$ and $500\,\text{pA}$.

considers the time elapsed since the last spike, it does not take into account the instantaneous state of the neuron, e.g. the voltage rate, as does Eq. (3). Hence, this type of approximation fails to account for spike timing during unsteady synaptic input. For example, as seen in Fig. 3, the thresholds for the first and following spikes of one spike train are equal, whereas the dynamic threshold approach from [13] would predict different values corresponding to the steady state, $t^* = \infty$, that is for the first spike, and to t^* equal to the appropriate interspike interval for the following spikes. In comparison, since Eq. (3) considers a local parameter of the state of the neuron, the voltage rate, it can describe the response to arbitrary stimulation.

2.3. Population density approach

To describe the activity of a population of similar neurons with common input current but different threshold potentials, we consider the probability density, ρ, which characterizes the number of neurons being in similar state of activity. Strictly speaking, ρ is the fraction of neurons per unit volume of the PS of neuron state parameters in the mathematical limit of an infinite number of neurons. As described, in order to avoid the complexity of a high-dimensional description we reduce our consideration to a one-dimensional version of the PS. Thus, we introduce the one-dimensional PS with the state variable, t^*, which for a neuron is the time elapsed since its last spike (Fig. 4). This
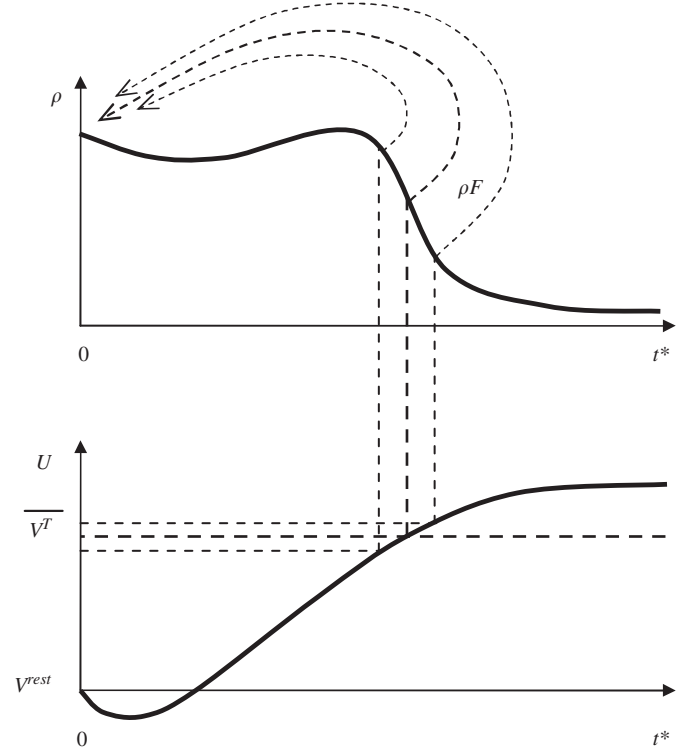

Fig. 4. The schematic representation of neuron evolution in the one-dimensional space of the time elapsed since the last spike. The density and voltage profiles are shown. Neurons move to the right till the next spike generation. After their spikes neurons transfer to the point $t^* = 0$.

PS is characterized by two-independent variables, t, the time, and t^*, the density being the dependent variable, $\rho = \rho(t, t^*)$. At any time t a small volume of the PS, $(t^*, t^* + \Delta t^*)$, contains the portion of neurons of a population, equal to $\rho(t, t^*)\Delta t^*$. The density $\rho(t, t^*)$ is referred to as refractory density in [11]. The value $\rho(t, 0)$ represents the firing rate of the ensemble. By the analogy with lagrangian and eulerian approaches in physics, we can consider the evolution of the density distribution by either tracing the coordinates (or t^*) of single particles (or neurons) or by calculating the fluxes of particles (neurons) passing by the fixed point (t^*). In the latter case we consider any function $f(t, t^*)$ as one of two-independent variables, t and t^*. To relate this function to a neuron with the "trajectory" $t^* = t^*(t)$, we formulate the rate of change by the so-called substantial derivative

$$\frac{df}{dt} = \frac{\partial f}{\partial t} + \frac{\partial f}{\partial t^*}\frac{dt^*}{dt}. \tag{4}$$

Trivially, up until the next spike the time since the previous spike is proportional to the time itself, i.e. $dt^*/dt = 1$. Thus,

$$\frac{df}{dt} = \frac{\partial f}{\partial t} + \frac{\partial f}{\partial t^*}. \tag{5}$$

To describe the temporal evolution of $\rho(t, t^*)$, we note that during periods in which the neurons do not fire the value of the refractory density at (t_1, t_1^*) would be equal to that at $(t_1 + \Delta t, t_1^* + \Delta t)$ with small Δt, i.e. $d\rho/dt = \partial\rho/\partial t + \partial\rho/\partial t^* = 0$. When neurons do fire, by definition they instantly move to the point $t^* = 0$. The rate of firing for neurons with some value of t^* is proportional to the density of neurons at that point, $\rho(t, t^*)$, and the probability for a single neuron to fire in a unit time, F. Thus, $d\rho/dt = -\rho F$. The function F is referred to in [11] as the hazard function or the spike-release probability density. Substituting the substantial derivative $d/dt = \partial/\partial t + \partial/\partial t^*$, we obtain that the evolution of ρ is governed by the transport equation with a source:

$$\frac{\partial\rho}{\partial t} + \frac{\partial\rho}{\partial t^*} = -\rho F. \tag{6}$$

To define the spike-release probability density, F, we first consider it to be a function of both U and $\overline{V^T}$, thus $F = F(U(t, t^*), \overline{V^T})$, i.e. the probability for a neuron to release a spike during the interval $[t, t + \Delta t]$, $F\Delta t$, depends on its subthreshold membrane potential $U = U(t, t^*)$ and on the distance to the threshold $\overline{V^T}$. This dependence implies comparison of U with the threshold potential $\overline{V^T}$ averaged over the ensemble, which has been calculated in Section 2.2.

The density ρ is normalized as follows:

$$\int_0^\infty \rho\, dt^* = 1. \tag{7}$$

As stated, when they spike neurons return to the point $t^* = 0$. This fact is reflected by the boundary condition for Eq. (6), which follows from Eq. (6) and the normalization

Eq. (7):

$$\rho(t, 0) = \int_{+0}^\infty \rho F\, dt^*. \tag{8}$$

As mentioned above, the value $\rho(t, 0)$ is the firing rate of the ensemble. In a stationary or quasi-stationary regime, $\rho(t, 0)$ corresponds to the firing rate of a single neuron with a mean threshold $\overline{V^T}$.

To define the membrane potential U for all t^*, we rewrite Eq. (2) by substituting the total derivative $d/dt = \partial/\partial t + \partial/\partial t^*$. Along with the equation for the potassium conductance, we get

$$C\left(\frac{\partial U}{\partial t} + \frac{\partial U}{\partial t^*}\right) = -I_K - I_L - I_i, \tag{9}$$

with

$$I_K = \overline{g}_K n(U - V_K), \quad \frac{\partial n}{\partial t} + \frac{\partial n}{\partial t^*} = \frac{n_\infty - n}{\tau_n}. \tag{10}$$

Approximations for $n_\infty = n_\infty(U)$, $\tau_n = \tau_n(U)$, can be taken from [24]. According to the threshold model described above, the voltage and the potassium conductance are constant during the latter half of the spike, i.e. $U(t, t^*) = U^{reset}$, $n(t, t^*) = n_K^{reset}$ for $0 < t^* < \Delta t_{AP}$, i.e. the boundary conditions for the Eqs. (9) and (10) at $t^* = \Delta t_{AP}$ are $U(t, \Delta t_{AP}) = U^{reset}$, $n(t, \Delta t_{AP}) = n_K^{reset}$.

We now define the function F, given the membrane potential U and its time derivative.

2.4. The spike-release probability density, F

A formula to calculate the spike-release probability density F should consider a model of noise and the variation of the cellular parameters over the entire neuron population. For the sake of simplicity, here we assume that the functional impact of these distributions may be expressed by a dispersion of the threshold potentials V^T over the population, and thus F may be expressed as $F = F(U, \overline{V^T})$, where $\overline{V^T}$ is the mean threshold value. To derive F, then, here we assume a Gaussian distribution of thresholds V^T, relative to the rest potential, with the mean value $\overline{V^T}$ and dispersion σ:

$$f^\sigma(V^T) = \frac{1}{\sqrt{2\pi}\sigma}\exp\left(-\frac{(V^T - \overline{V^T})^2}{2\sigma^2}\right).$$

Hence, the function $F = F(U, \overline{V^T})$ can be derived from its definition, Eq. (6), i.e. $F = -(1/\rho)/(d\rho/dt)$. For simplicity, we analytically consider the case of a gradually increasing potential, $U(t)$, in an ensemble of neurons which all have identical stimulation. At the beginning of the stimulation $\overline{\rho(0)} = \rho_0$, $U(0) = V^{rest}$. For a given value of $U(t)$, the threshold model gives the density $\rho(t) = \rho_0(1 - \int_{-\infty}^{U(t) - V^{rest}} f^\sigma(V^T)\, dV^T)$. Using the Eq. (6) for the total
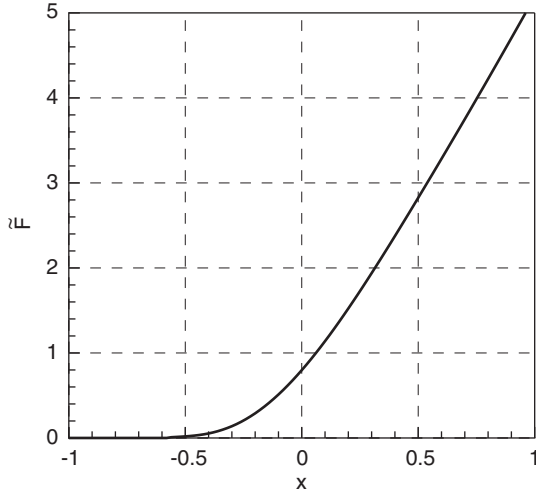
Fig. 5. The dimensionless function $\tilde{F}(x)$ defined by Eq. (11) is shown, characterizing how the probability for a neuron to fire changes with the dimensionless potential x compared to the threshold value $x = 0$.

derivative of time, we obtain

$$F = -\frac{1}{\rho}\frac{d\rho}{dt} = -\frac{1}{\rho}\frac{\partial\rho}{\partial U}\frac{dU}{dt} = \frac{dU}{dt}\frac{f^\sigma(U(t) - V^{\text{rest}})}{1 - \int_{-\infty}^{U(t) - V^{\text{rest}}} f^\sigma(V^{\text{T}})\,dV^{\text{T}}}.$$

Substituting the Gaussian distribution of $\overline{V^{\text{T}}}$, we get the spike-release probability density $F(U, \overline{V^{\text{T}}})$
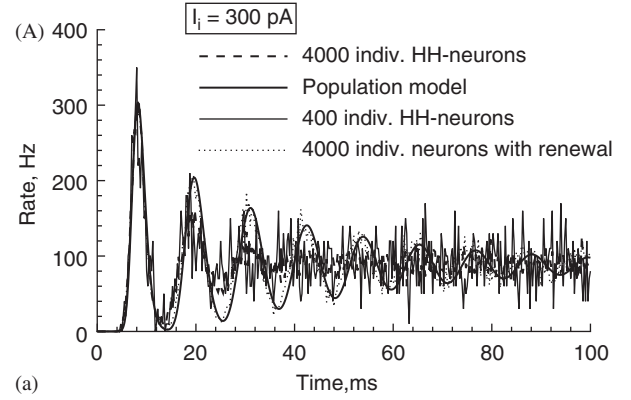
$$F(U, \overline{V^{\text{T}}}) = \frac{dU}{dt}\frac{1}{\sigma}\tilde{F}\left(\frac{U - V^{\text{rest}} - \overline{V^{\text{T}}}}{\sqrt{2}\sigma}\right), \tag{11}$$
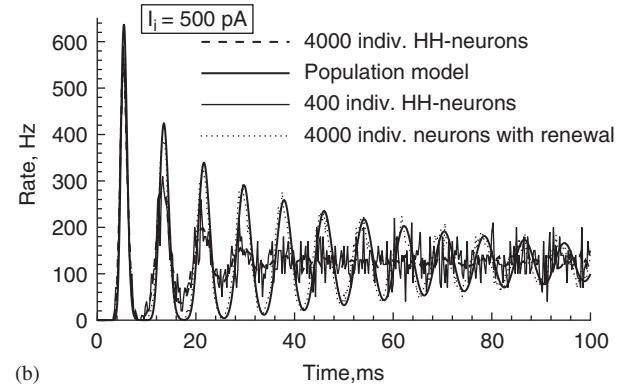
where

$$\tilde{F}(x) = \sqrt{\frac{2}{\pi}}\frac{\exp(-x^2)}{1 - \text{erf}(x)}.$$

The obtained dimensionless function $\tilde{F}(x)$ is shown in Fig. 5. This function characterizes how the firing probability of a neuron depends on the dimensionless potential x compared to the threshold value $x = 0$.
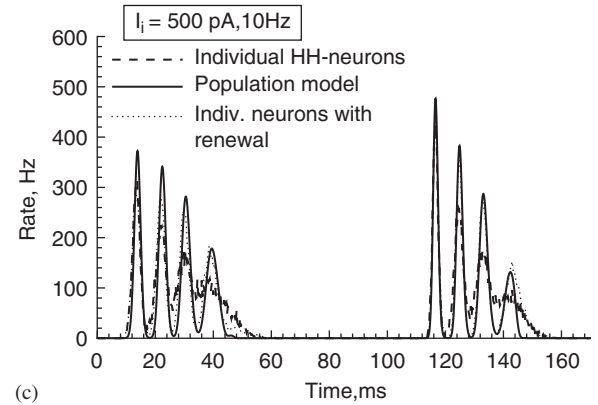
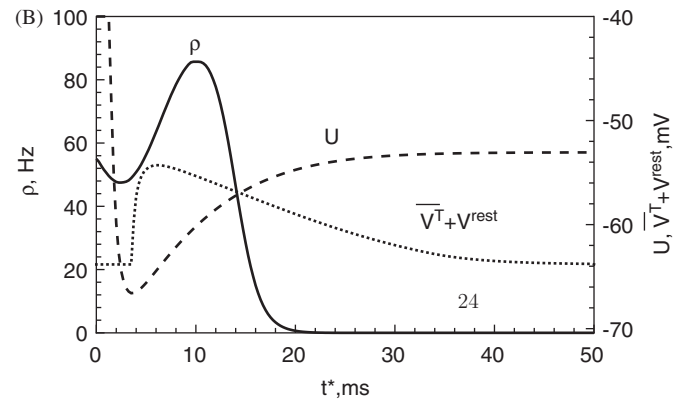Thus, we obtain a system of Eqs. (3), (6), (8)–(11) governing the activity of a neuronal ensemble.

Fig. 6. The transient response of the population firing rate to a rapid change in input. (A) Beginning at $t = 0$, the excitatory input current to the uncoupled neurons of a single population stepped up to 300 and 500 pA, correspondingly in a and b. The firing rate transiently jumps up before returning to a new steady-state response. The population model firing rate (solid line) compares with the averaged firing rate of individual Hodgkin–Huxley neurons. Two cases with and without renewal of the dispersed thresholds after the spikes are shown in the dotted and dashed lines, correspondingly. In Ac the responses to oscillating input current of 500 pA amplitude and 10 Hz frequency are shown for the same models as in Aa, b. (B) Distributions of the potential $U(t^*)$ and density $\rho(t^*)$ across the time elapsed since the last spike, at the time moment $t = 100$ ms, corresponding to Aa.

3. Results: population and individual neuron simulations

In this section, we present simulations for a population of uncoupled neurons, and simulations for a population of coupled neurons, in both cases where all the neurons receive the identical input from an external source. For all simulations the threshold potentials are normally dispersed with the dispersion $\sigma = 2\,\text{mV}$. We compare the population density approach with the direct simulation of a population of individual neurons.

The population density equations were solved numerically using the finite-difference total variation diminishing (TVD) scheme [12] with second order approximations in both directions of the independent coordinates. In response to a rapid change in input, the firing rate transiently jumps up before returning to a new steady-state response (Fig. 6A). The distributions of the potential U and the density ρ in the PS at one instant in time are shown in Fig. 6B. The steep gradient of the density corresponds to near-threshold potentials.

The population density represents the fraction of neurons per unit time t^* in the mathematical limit of an infinite number of neurons. Thus for the direct simulations of explicit neurons we considered a large population of Hodgkin–Huxley neurons and compared their dynamics with the predictions from the population density approach. As an analog to the threshold variability defined in the population density approach, in the explicit simulations the midpoint of the sodium channel steady-state activation characteristic $m_\infty(V)$ for each neuron was taken at random from a Gaussian distribution with a dispersion $\sigma = 2\,\text{mV}$. Numerical results were obtained using 4000 neurons for the direct simulation and using 200 nodes in the population approach, corresponding to the discretization in the t^*-space. As seen in Fig. 6A the simulated rates of the individual neuron models and of the population model are similar. The timing and amplitude of the first maximum are well reproduced by the population model. The discrepancy in the following peaks is mainly due to the implicit renewal assumption taken for the spike-release probability function in the population model. Thus after each spike a new threshold value of a neuron in population model is independent of its value before the spike. In comparison, each individual neuron of the explicit simulation keeps its threshold value that was determined prior to the simulation. As a result, a neuron with a low threshold fires earlier and earlier at every peak of the population firing rate, and likewise one with a high-threshold fires later and later at every peak, resulting in a greater dissipation of the firing times over the population as a whole.

To verify this interpretation, we considered an alternative model of the neural parameter distribution in the direct simulations. Thus, we assumed a renewal process for the midpoint of the $m_\infty(V)$ after each spike for each neuron, chosen from the same Gaussian distribution. This model is similar to so-called slow-noise models, as described in [11]. In this case the firing rate calculated by the proposed population model and by the direct simulations coincide, as shown in Fig. 6Aa,b by the dotted lines.

We next demonstrate the ability of the proposed model to respond to more complex stimulation, applying a sinusoidal input current with an amplitude of 500 pA and frequency 10 Hz (Fig. 6 Ac). Comparison of the rates of the individual neurons in direct simulations and of the population model shows similar responses, with population spikes at the peaks of the stimulating current. As in the previous examples, the match between the population model and the pooled activity of the individual neuron models improves when the latter incorporates a renewal process for the voltage dependence of the sodium channel activation. The remaining discrepancy between the approaches arises primarily for the following two reasons. First, the precision of the single parameter approximation for the threshold potential, dependent on the potential rate, is limited. Second, the sensitivity of the membrane potential to the input just prior to a spike is different between the Hodgkin–Huxley and threshold neuron models, due to the sub-threshold activation of the sodium channel in the former.

The proposed formulation may also be applied for synaptically connected networks. To demonstrate this point we simulate the activity of a recurrent interneuron network including all-to-all connectivity by inhibitory synapses. In this case the input current consists of two terms, $I_i(t) = I_{\text{ext}}(t) + I_S(t)$. The first term, I_{ext}, is the applied external current, taken to be 500 pA and starting at $t = 0$ in Fig. 6Ab. The second term $I_S(t)$ is the synaptic current governed by the population firing rate, i.e.

$$I_S(t) = g_S(t)(U(t) - V_S), \tag{12}$$

$$\tau_S^2 \frac{d^2 g_S(t)}{dt^2} + 2\tau_S \frac{dg_S(t)}{dt} + g_S(t) = \overline{g}_S v(t - \tau_d), \tag{13}$$

where $v(t)$ is the population firing rate, here expressed as number of spikes per unit time (ms). As noted previously for the population model $v(t)$ is given as $\rho(t, 0)$, whereas for the direct simulation $v(t)$ is given by the number of spikes per unit time, normalized over the total number of neurons. The remaining terms are equivalent for the two models: τ_S is the synaptic time constant, τ_d is the synaptic delay, $\overline{g}_S$ is the maximum synaptic conductance, and V_S is the synaptic current reversal potential. For purposes of illustration the following values were used here: $\tau_S = 3\,\text{ms}$, $\tau_d = 1\,\text{ms}$, $V_S = -80\,\text{mV}$, $\overline{g}_S = 7\,\text{ms/cm}^2$. As shown in Fig. 7 the population model shows quite similar behavior to simulations of a recurrent network made of explicit individual neurons. The mismatch in this case is due to the reasons mentioned above for the case of oscillatory input, but here amplified by the feedback term given by the synaptic integration. In contrast to the uncoupled neuron population (Fig. 6Ab), the recurrent network passes from the transient activity into the steady-state oscillations. We propose that these oscillations relate to the physiological gamma-oscillations, given that one suggested mechanism
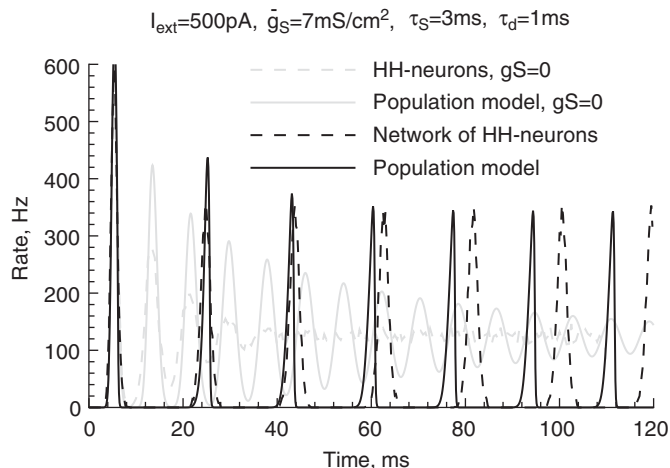
Fig. 7. The oscillatory response of the recurrent inhibitory neuron network to the input current stepped up to 500 pA. The synaptic current is given by the Eq. (12). The solutions obtained by the population model (solid) and by direct simulation (dashed) are shown. To compare, the solutions for the uncoupled neuron population are shown in gray lines.

of gamma-oscillations involves an inhibitory neural population undergoing tonic excitation [16,22,25]. The resulting oscillatory activity of the interneurons, as represented by the network modeled here, is reflected in the recorded activity of principal excitatory cells.

4. Discussion

A novel modification of the population density method has been proposed for modeling large groups of neuron. The method is simple yet captures the main details of the dynamics of real neurons and networks, namely, the refractoriness due to the sub-threshold influence of the potassium current, a dynamic threshold for action potentials, and the impact of variability in intrinsic cell properties and in synaptic input. Here we outline the advantages of the model and its possible extensions.

Previous population density approaches for studying the dynamics of neuronal populations have considered distributions of neurons across either the membrane voltage or the time passed since the last spike. The former method has been based on the integrate-and-fire neuron [17,11,1,18,3,10]. The latter method, that is the refractory density approach, is based on the SRM [9,11,2,15]. As a more general single-neuron model than the integrate-and-fire neuron, the SRM can more precisely describe the neuron dynamics. Moreover, in contrast to the membrane potential, the time since the last spike monotonically changes with time (modulo spike times) and better describes the state of a neuron, in particular, its refractory properties. Although in general the input to a neuron is composed of a current term and a conductance term [19], the SRM considers only input current [11,15], and thus the shunting effect of the input is neglected.

The refractory density approach proposed in the present paper is based on a single-neuron model which is different from the SRM. The SRM supposes that the membrane potential is a sum of a term reflecting the evoked spike and a postsynaptic term reflecting the synaptic input. The parts are constructed to be independent to obtain a unique sub-threshold voltage curve for a set of neurons with different thresholds. In contrast, the present paper states that instead of the decomposition it is sufficient to omit the sodium current when calculating the potential relative to the spike threshold. As a consequence, the approach has several advantages to the SRM-based RDE approach and other known one-dimensional population models. First, the threshold calculated as a one-parametric dependence on the potential slope provides better accuracy because it implicitly reflects the activity of the omitted sodium channels. Second, using the current approach it is possible to take into account additional fast ionic currents as well as slow currents averaged over the cell population [6], due to the explicit conductance-based formulation of the approach. Third, the spike-release probability density function *F*, or "hazard function", directly follows from the RDE and assumed (here, Gaussian) distribution of thresholds in neurons. Finally, the current model is described by partial differential equations, which are easier to solve than integral–differential equations such as used in [11,17].

The single-neuron conductance-based model at the heart of the method proposed here can be explicitly matched to experiment. Since, as shown, the proposed threshold model well reproduces the sub-threshold voltage and the spike times of the full neuron model, it is well suited as well to model an experimentally recorded neuron. Moreover, the σ dissipation parameter of the refractory density model can be directly estimated from repeated experimental trials of spike trains in one or many neurons. It should be pointed out that in the present paper the single-neuron model was taken as known from [24], thus the threshold dependence on potential slope and the spike reset parameters were directly measured from the full neuron model. In the density equations evaluated here, as well, the threshold dispersion σ was fixed to a reasonable value and thus was not adjusted in order to provide a better match to the direct simulations. Hence, particularly, the situation considered here with the stimulation of the current step response is not the special case for the model.

The computational efficiency of the population modeling in the framework of the density equation is significantly better than that of the direct simulation of explicit individual neurons. In particular, for the proposed model this follows as it belongs to the class of one-dimensional density equation approaches, for which estimations of computation efficiency can be found in [17,11]. These results, which are consistent with our observations for the simulations presented here, demonstrate that the population density approach is between 10 and 100 times faster than the individual neuron simulations.

Thus, the proposed approach provides certain advantages when used as the core of a model of cortical tissue activity. For example, a two-population model of hippocampal CA1 has been constructed by the authors [6], which simulates extracellularly stimulated postsynaptic responses in neurons, as well as gamma-oscillations. The extensions made for the model to be fitted to the experiments are as follows: (i) A novel two-compartment cellular model has been proposed [7] to coordinate voltage clamp with current clamp whole-cell patch recordings in cortical slices. In contrast to the known Pinsky–Rinzel model, the proposed model uses somatically measured synaptic currents which makes it more applicable to the population approach. (ii) The somatic synaptic currents I_i have been approximated by a second order differential equation with a presynaptic firing rate as a source term. There is a robust correspondence between the two-exponential curve and the somatically measured synaptic current in response to a brief stimulus for different types of dendritic trees and synapse populations. (iii) The AHP-current has been taken into account for a population of pyramidal cells, considering AHP-conductance as being governed by the firing rate. (iv) Finally, to consider the spatial propagation of neural activity, such as traveling waves, the wave-like hyperbolic partial differential equation [14] has been applied in [4], which treats only local connections, in terms of somatic and pre-synaptic firing rates. Coupled with the remaining equations, the approach predicts traveling waves moving with a velocity dependent on the ratios of synaptic strengths.

In summary, in this paper we develop a refractory density approach using a threshold conductance-based neuron model. The proposed approach provides certain advantages over previously developed refractory density approaches based on a SRM. The model of a single population of neurons demonstrated here can be used as a core of a population model of cortical tissue, that can be quantitatively fitted to intracellular experimental data recordings. The reduced evaluation time of the proposed refractory density approach should facilitate modeling more complex neural networks, as compared to the evaluation of networks based on explicit individual neuron models. Thus, the refractory density approach may be an important tool for the implementation of truly large-scale models of the networks in the brain.

Acknowledgment

References

[1] L.F. Abbott, C. van Vreeswijk, Asynchronous states in a network of pulse-coupled oscillators, Phys. Rev. E 48 (1993) 1483–1490.

[2] H.U. Bauer, K. Pawelzik, Alternating oscillatory and stochastic dynamics in a model for a neuronal assembly, Physica D 69 (1993) 380–393.

[3] N. Brunel, V. Hakim, Fast global oscillations in networks of integrate-and-fire neurons with low firing rates, Neural Comput. 11 (1999) 1621–1671.

[4] A.V. Chizhov, Model of populational activity of hippocampal neurons, in: Proceedings of the 2001 International Symposium on Nonlinear Theory and its Applications, Zao, Japan, 2001, pp. 23–26.

[5] A.V. Chizhov, Model of evoked activity of hippocampal neuron populations, Biophysics 47 (6) (2002) 1007–1015.

[6] A.V. Chizhov, The model of neuron populations as a unit of a large-scale network, Neurocomput. Design Appl. 2–3 (2004) 60–68.

[7] A.V. Chizhov, A two-compartmental model for the dependence of a postsynaptic potential on a postsynaptic current, measured by patch-clamp, Biophysics 49 (5) (2004) 877–880.

[8] P. Dayan, L.F. Abbott, Theoretical Neuroscience, MIT Press, Cambridge, MA, 2001.

[9] J. Eggert, J.L. van Hemmen, Modeling neuronal assemblies: theory and implementation, Neural Comput. 13 (2001) 1923–1974.

[10] S. Fusi, M. Mattia, Collective behavior of networks with linear (vlsi) integrate and fire neurons, Neural Comput. 11 (1999) 633–652.

[11] W. Gerstner, W.M. Kistler, Spiking Neuron Models Single Neurons, Populations, Plasticity, Cambridge University Press, Cambridge, 2002.

[12] A. Harten, S. Osher, Uniformly high-order accurate non-oscillatory schemes I, SIAM J. Numer. Anal. 24 (2) (1987) 279–309.

[13] S. Hill, G. Tononi, Modeling sleep and wakefulness in the thalamocortical system, J. Neurophysiol. 8 (2005) 1671–1698.

[14] V.K. Jirsa, H. Haken, A field theory of electromagnetic brain activity, Phys. Rev. Lett. 77 (1996) 960–963.

[15] R. Jolivet, T.J. Lewis, W. Gerstner, Generalized integrate-and-fire models of neuronal activity approximate spike trains of a detailed model to a high degree of accuracy, J. Neurophysiol. 92 (2) (2004) 959–976.

[16] R. Khazipov, G.L. Holmes, Synchronization of Kainate-induced epileptic activity via GABAergic inhibition in the superfused rat hippocampus in vivo, J. Neurosci. 23 (12) (2003) 5337–5341.

[17] D. Nykamp, D. Tranchina, A population density approach that facilitates large-scale modeling of neural networks: analysis and application to orientation tuning, J. Comput. Neurosci. 8 (2000) 19–50.

[18] A. Omurtag, B.W. Knight, L. Sirovich, On the simulation of large populations of neurons, J. Comput. Neurosci. 8 (2000) 51–63.

[19] A.N. Pokrovskii, Effect of synapse conductivity on spike development, Biofizika 23 (4) (1978) 649–653.

[20] P.A. Robinson, C.J. Rennie, J.J. Wright, Propagation and stability of waves of electrical activity in the cerebral cortex, Phys. Rev. E 56 (1997) 826–841.

[21] O. Shriki, D. Hansel, H. Sompolinsky, Rate models for conductance-based cortical neuronal networks, Neural Comput. 15 (2003) 1809–1841.

[22] R.D. Traub, M.A. Whittington, S.B. Colling, G. Buzsaki, J.G. Jefferys, Analysis of gamma rhythms in the rat hippocampus in vitro and in vivo, J. Physiol. 493 (2) (1996) 471–484.

[23] A.A. Turbin, A.V. Chizhov, Model of neuronal ensemble, in: Proceedings of the Conference on Neuroinformatics-2003, Moscow, 2003, pp. 133–140 (in Russian).

[24] J.A. White, C.C. Chow, J. Ritt, C. Soto-Trevino, N. Kopell, Synchronization and oscillatory dynamics in heterogeneous, mutually inhibited neurons, J. Comput. Neurosci. 5 (1998) 5–16.

[25] M.A. Whittington, R.D. Traub, J.G. Jefferys, Synchronized oscillations in interneuron networks driven by metabotropic glutamate receptor activation, Nature 373 (6515) (1995) 612–615.

[26] M.N. Zhadin, Formation of rhythmic processes in the bioelectrical activity of the cerebral cortex, Biophysics 39 (1) (1994) 129–147.

Anton V. Chizhov received his Ph.D. in 1998 from the Physico-Mechanical Department at the St.-Petersburg State Polytechnic University and the A.F. Ioffe Phisico-Technical Institute, in computational fluid dynamics. His research interests include biophysically detailed models of neurons and cortical neural tissue, estimation of network parameters from intracellular electrophysiological recordings.

Andrey A. Turbin received his M.Sc. in physics in 2002, and Ph.D. in physics–mathematics in 2005 from the Radio-Physics Department at the St.-Petersburg State Polytechnic University. His research interests include neural networks modeling, phase approach in realistic neurons modeling, Hodgkin–Huxley equation, programming.

Lyle J. Graham received his Ph.D. in medical engineering/medical physics from Harvard Medical School and the Massachusetts Institute of Technology. His group in the CNRS focuses on the biophysical mechanisms and synaptic circuitry underlying functional properties in the visual system and hippocampus. His approach combines in vivo and in vitro intracellular electrophysiological recordings for measuring intrinsic properties of neurons and the synaptic dynamics during evoked responses, with quantitative analysis that relies on biophysically detailed and formal models of neurons and their networks.